

# Monitoring and rapid quantification of total carotenoids in *Rhodotorula glutinis* cells using laser tweezers Raman spectroscopy

Zhanhua Tao<sup>1</sup>, Guiwen Wang<sup>1</sup>, Xiaodong Xu<sup>1</sup>, Yufeng Yuan<sup>1,2</sup>, Xue Wang<sup>1,2</sup> & Yongqing Li<sup>3</sup>

<sup>1</sup>Laboratory of Biophysics, Guangxi Academy of Sciences, Nanning, China; <sup>2</sup>Department of Physics, Guangxi Normal University, Guilin, China; and <sup>3</sup>Department of Physics, East Carolina University, Greenville, NC, USA

**Correspondence:** Zhanhua Tao, Laboratory of Biophysics, Guangxi Academy of Sciences, Nanning, Guangxi 530003, China. Tel.: +867 712 503 995; fax: +867 712 503 932; e-mail: taozhanhua@hotmail.com

Received 12 September 2010; revised 8 October 2010; accepted 9 October 2010.  
Final version published online 8 November 2010.

DOI:10.1111/j.1574-6968.2010.02139.x

Editor: Aharon Oren

## Keywords

Raman spectroscopy; optical tweezers; carotenoids; *Rhodotorula glutinis*.

## Abstract

*Rhodotorula glutinis* is known to accumulate large amounts of carotenoids under certain culture conditions, which have very important industrial applications. So far, the molecular mechanism of regulating carotenogenesis is still not well understood. To better understand the carotenogenesis process, it requires methods that can detect carotenogenesis rapidly and reliably in single live cells. In this paper, a method based on laser tweezers Raman spectroscopy (LTRS) was developed to directly detect carotenoids, as well as other important biological molecules in single live *R. glutinis* cells. The data showed that the accumulation of carotenoids and lipids occurred mainly in the late exponential and stationary phases when the cell growth was inhibited by nutrient limitation. Meanwhile, the carotenoid concentration changed together with the concentration of nucleic acids, which increased in the first phase and decreased in the last phase of the culture. These data demonstrate that LTRS is a rapid, convenient, and reliable method to study the carotenogenesis process *in vivo*.

## Introduction

Carotenoids represent a group of important natural pigments widely used in the pharmaceutical, cosmetic, food, and feed industries. The biological sources of carotenoids have received more attention because they have lower toxicity and higher bioavailability than their chemically synthesized counterparts. Several microorganisms, including bacteria, algae, molds, and yeasts, are able to produce carotenoids. Among these microorganisms, yeasts such as *Phaffa rhodozyma* and *Rhodotorula glutinis* are of commercial interest due to their unicellular nature and high growth rate. *Rhodotorula glutinis* can produce carotenoids when the cell is under stress, such as nutrient limitation (Simpson *et al.*, 1964). Carotenoid content in wild strains of *R. glutinis* is relatively low for industrial purposes, and efforts have been made to increase the carotenoid content through strain improvement (Bhosale & Gadre, 2001a) and optimization of the culture condition (Wang *et al.*, 2007). Recently, Frengova & Beshkova (2009) reviewed the factors affecting carotenogenesis in the yeast *Rhodotorula*. However, the molecular mechanism of carotenogenesis regulation is still not well understood.

The conventional methods for quantifying the total carotenoid level in microorganisms involve UV (Tereshina *et al.*, 2003) or HPLC (Kaiser *et al.*, 2007) measurement after organic solvent extraction. However, the extraction step may cause degradation or isomerization of carotenoids, affecting the measurements. In addition, the *in vitro* methods based on solvent extraction can only obtain information regarding the averaging effect of a population of cells. To better understand the regulation of carotenogenesis, it requires the development of rapid, convenient, and reliable methods, which could quantify the carotenoid content in live cells.

In recent years, Raman spectroscopy has been widely applied in biological fields like disease diagnosis (Kanter *et al.*, 2009), tissue engineering (Nottingham *et al.*, 2003), microorganism identification (Buijters *et al.*, 2008), and protein conformation determination (Rousseau *et al.*, 2004). The main drawback of the traditional confocal Raman microscopy is that the target cell must be immobilized by physical or chemical approaches. Combining Raman microscopy with optical tweezers makes it possible to analyze single, live, moving cells in medium. This new combined technique, called confocal laser tweezers Raman

spectroscopy (LTRS), has been extensively used in studies of optically trapped chromosomes (Ojeda *et al.*, 2006), spores (Huang *et al.*, 2007), *Escherichia coli* cells (Chen *et al.*, 2009), and mitochondria (Tang *et al.*, 2007).

Raman spectroscopy is extraordinarily sensitive to the detection of carotenoids, especially when using an excitation wavelength resulting in the resonance Raman effect, most frequently that at 514.5 nm (Vitek *et al.*, 2009). On the other hand, photodamage may occur for living cells when using the 514.5 nm wavelength for excitation (Snook *et al.*, 2009). The use of a longer wavelength, such as near-infrared wavelength, can substantially decrease the photodamage effect (Ashkin *et al.*, 1987). Raman spectroscopy has been reported to detect carotenoids from intact plants (Baranski *et al.*, 2005), human retina (Bernstein *et al.*, 1998), and fungal pellet (Papaioannou *et al.*, 2009). However, most of the investigations have been performed at the tissue level, and thus do not permit further understanding of the carotenoid accumulation process in unicellular microorganisms, such as *R. glutinis*. These single cell analysis techniques can help to get more information, which might be buried during bulk measurements.

In this paper, we developed a method based on LTRS to carry out rapid, real time measurements of the total carotenoids, as well as nucleic acids and lipids inside single *R. glutinis* cells. The LTRS technique permits the capture of a single cell suspended in a solution in the focus of a near-infrared laser beam and the subsequent analysis of this cell using Raman spectroscopy, from which the levels of carotenoids can be determined from the intensity of the 1509 cm<sup>-1</sup> band in Raman spectra.

## Materials and methods

### Microbial strains, culture conditions, and preparation of the sample

The strain of *R. glutinis* was kindly provided by Ms. Lianzhu Teng at Guangxi University. Single colonies of *R. glutinis* from YPD plates (containing 10 g of yeast extract, 20 g of peptone, 20 g of dextrose, and 15 g of agar L<sup>-1</sup>) were inoculated into a liquid YPD medium (containing no agar) and incubated at 28 °C for 16 h to obtain the preculture. The preculture in exponential phase was used as the inoculum for 50 mL of carotenoid production medium. The production medium was composed of dextrose (40 g L<sup>-1</sup>), KH<sub>2</sub>PO<sub>4</sub> (8 g L<sup>-1</sup>), MgSO<sub>4</sub>·7H<sub>2</sub>O (0.5 g L<sup>-1</sup>), and yeast extract (5 g L<sup>-1</sup>), with a final pH of 6.0. The inoculum was placed in a 250 mL shaking flask, shaken at 200 r.p.m., and incubated at 28 °C for 72 h. A 500-μL aliquot of cells was withdrawn at 4-h intervals to measure growth and collect Raman spectra.

## Experimental setup and Raman measurements

Details of the LTRS method have been published elsewhere (Xie *et al.*, 2002, 2005). A circularized beam from a diode laser at 780 nm was spatially filtered and then introduced into an inverted microscope (Nikon TE2000U) equipped with an objective (×100, NA 1.30) to form a single-beam optical trap. A *R. glutinis* cell in the phosphate-buffered saline (PBS) was trapped about 10 μm above the bottom of cover slip with a gradient force generated by the focused beam. The same laser beam was used to excite Raman scattering from molecules inside the trapped cell. The spectrum was obtained by a liquid-nitrogen-cooled charge-coupled detector. The spectral resolution of our Raman system was about 6 cm<sup>-1</sup>. The Raman measurement of an individual cell was performed with a 10-s exposure time and 30 mW excitation power. The Raman spectra of 100 cells were collected for each time point. The PBS background spectrum was recorded with the same acquisition condition without the trapped cells and subtracted from the spectra of individual cells. The subtracted spectra were then smoothed using the Adjacent-Averaging filter method. Preprocessing of spectral data was performed using MATLAB 7.0 software. The total carotenoid level in an individual cell was estimated from the peak intensity at 1509 cm<sup>-1</sup> in its Raman spectrum.

### Preparation of β-carotene standard curve

β-Carotene standard (purchased from Sigma-Aldrich) was dissolved in chloroform and diluted into a series of concentrations: 62.5, 125, 187.5, 250, 312.5, 375, 437.5, and 500 mg L<sup>-1</sup>. For each measurement, a 150-μL aliquot of β-carotene solution was added to the sealed holder and its Raman spectrum was acquired with the same experimental parameters used for determining the cell spectra. The Raman spectrum of the pure chloroform was taken as background and subtracted from the above-mentioned spectra. A standard curve for carotenoid quantification was linearly fitted by correlating the β-carotene concentration with the peak intensity at 1518 cm<sup>-1</sup> in its Raman spectrum.

## Results and discussion

### Quantitative analysis of carotenoids in live *R. glutinis* cells using LTRS

Carotenoids are a family of isoprenoids containing a characteristic polyene chain of conjugated double bonds. In *R. glutinis* cells, carotenoid pigments predominantly consist of β-carotene, torulene, and torularhodin (Sakaki *et al.*, 2002). In this work, the Raman spectra of *R. glutinis* cells cultivated for 12 and 32 h, as well as the pure β-carotene standard were acquired in order to verify the existence of carotenoids in the investigated strain (Fig. 1). The three fundamental

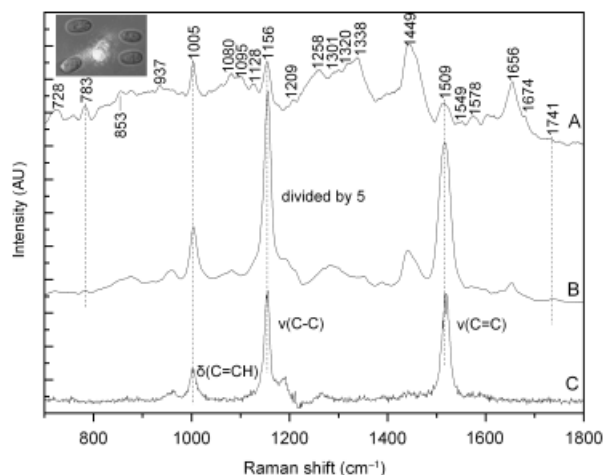


**Fig. 1.** Raman spectra of *Rhodotorula glutinis* cells and  $\beta$ -carotene standard. The spectra are average from 100 cells cultured for 12 h (curve A) and 32 h (curve B, divided by a factor of 5);  $25 \text{ mg L}^{-1}$   $\beta$ -carotene solution (curve C). For all measurements, the laser power was 30 mW at 780 nm and the data acquisition time was 10 s. The inset shows the image of *R. glutinis* cells under trapping and measuring.

carotenoid bands at  $1505\text{--}1520 \text{ cm}^{-1}$  assigned to  $\text{C}=\text{C}$  ( $\nu_1$ ) in-phase stretching,  $1156 \text{ cm}^{-1}$  assigned to  $\text{C}-\text{C}$  ( $\nu_2$ ) stretching and  $1005 \text{ cm}^{-1}$  assigned to  $\delta(\text{C}=\text{CH})$  in-plane rocking modes of  $\text{CH}_3$  groups were clearly visible in all of the spectra. Thus, to a high degree of certainty, these peaks resulted from carotenoid compounds. The intensity of these peaks for *R. glutinis* cells cultivated for 32 h was more than 30 times higher than those for cells cultivated for just 12 h. It is noteworthy that the  $\text{C}=\text{C}$  ( $\nu_1$ ) peak was at  $1509 \text{ cm}^{-1}$  for carotenoids present in cells, while it was at  $1518 \text{ cm}^{-1}$  for the  $\beta$ -carotene standard. This difference may be attributed to the fact that carotenoids usually bind to proteins or lipids in *R. glutinis* cells and the  $\text{C}=\text{C}$  ( $\nu_1$ ) wave number is significantly influenced by carotenoid interaction with other molecules inside the cells (Schulz *et al.*, 2005). Apart from the above peaks assigned to carotenoids, peaks associated with nucleic acids (located at 728, 783, 1095, 1338, and  $1578 \text{ cm}^{-1}$ ), proteins (located at 1005, 1080, 1209, 1258, and  $1656 \text{ cm}^{-1}$ ), and lipids (located at 1301 and  $1741 \text{ cm}^{-1}$ ) were also observed in the Raman spectra of *R. glutinis* cells cultivated for 12 and 32 h (these peaks were not as clear in Fig. 1b as in Fig. 1a, for Fig. 1b had been divided by a factor of 5 to match Fig. 1a and Fig. 1c). This provided abundant information regarding the composition and structure of intracellular molecules of *R. glutinis* cells. The major peak assignments for *R. glutinis* cells are shown in Table 1.

Because the amount of Raman scattered light solely depends on the molecules found in the sample and environment, the intensity of the Raman bands for carotenoids should correlate linearly with the carotenoid concentration.

**Table 1.** *Rhodotorula glutinis* cell Raman band assignments

Peak position ( $\text{cm}^{-1}$ )	Assignment	Reference
728	A	(1), (2), (3)
783	C, T/DNA: O-P-O <sup>-</sup>	(1), (2), (3)
853	p: Ring br. Tyr	(1), (2), (3)
937	p: C-C bk. $\alpha$ helix	(1), (3)
1005	p: Phe/car: $\text{CH}_3$ rock	(1), (2), (4)
1080	p: C-N str.	(1)
1095	DNA: O-P-O <sup>-</sup>	(1), (2), (3)
1128	p: C-N str.	(1), (3)
1156	p: C-C/C-N str./car: C-C str.	(1), (4)
1209	C-C <sub>6</sub> H <sub>5</sub> str. Phe, Trp	(1), (2)
1258	p: Amide III $\beta$ sheet	(1), (2)
1301	Lipids: CH <sub>2</sub> twist	(1)
1320	G/p: CH def	(1), (3)
1338	A, G def/p: CH def	(1), (2), (3)
1449	Lipids/p: CH def	(1), (3)
1509	car: C=C str.	(4)
1549	G	(2)
1578	G, A	(1), (2), (3)
1656	p: Amide I $\alpha$ helix	(1), (2)
1674	T: C=O/p: Amide I $\beta$ sheet	(2), (5)
1741	Lipid: > C=O ester	(1)

1, Notingham *et al.* (2003); 2, Xu (2005); 3, Xie *et al.* (2007); 4, Vitek *et al.* (2009); 5, Li-Chan (1996).

A, adenine; G, guanine; C, cytosine; T, thymine; def, deformation; Phe, phenylalanine; str., stretching; br., breathing; bk, backbone; car, carotenoids; p, proteins.

However, among three of the main Raman bands for the carotenoids, the  $\text{C}=\text{C}$  ( $\nu_1$ ) intensity is significant and there are no peaks from the other intracellular components in the vicinity of  $\text{C}=\text{C}$  ( $\nu_1$ ). Therefore, this peak may be the best choice for estimation of the carotenoid concentration. To establish the relationship between  $\text{C}=\text{C}$  ( $\nu_1$ ) intensity and carotenoid concentration, we determined the  $\text{C}=\text{C}$  ( $\nu_1$ ) peak intensity for a series of diluted  $\beta$ -carotene solution. The data were linearly fitted ( $R^2 = 0.9982$ ; Fig. 2), and can be used as the standard curve for  $\beta$ -carotene quantification. Because the  $\text{C}=\text{C}$  ( $\nu_1$ ) intensity is mainly dependent on the polyene chain present in all of the carotenoids (substituent groups have a minor effect), the total carotenoid content can be directly estimated using the standard curve in future experiments.

### Kinetics of carotenoid content during the culture process

For a batch culture of *R. glutinis*, the aeration, constituents, and pH value of the culture medium vary throughout the culture process. Cells growing under different environmental conditions will contain different amount of biological molecules, which would generate their own Raman signals. Monitoring the changes of the amount of biological

molecules within cells using Raman spectroscopy may increase our knowledge of substance metabolism for living cells. Figure 3a shows the growth curve of *R. glutinis* and the profile of carotenoid accumulation inside *R. glutinis* cells in a batch culture. The cellular growth was monitored by measuring the OD at 600 nm. At each time point, Raman spectra of 100 randomly selected individual cells were acquired. The carotenoid content within an individual cell was estimated using the equation for the standard curve mentioned above. Because the preculture used as inoculum had grown in YPD broth for 16 h before inoculation, some carotenoids should have accumulated inside cells when they were transferred to the fresh carotenoid production medium. The carotenoids formed during preculture decreased rapidly soon after inoculation, and remained at a low level in the early exponential phase (8–24 h). Some carotenoid accumulation occurred from 28 to 44 h, and the maximum

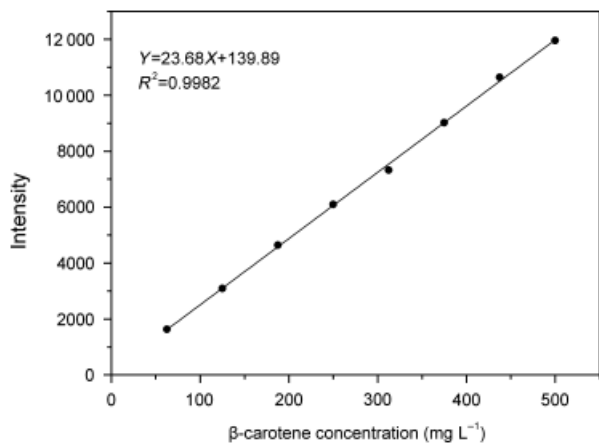


**Fig. 2.** Correlation between the C=C ( $\nu_1$ ) peak intensity and the  $\beta$ -carotene concentration.

carotenoid production rate was observed in the late exponential phase and the stationary phase (48–60 h), with an average rate of  $40 \text{ mg L}^{-1} \text{ h}^{-1}$ . The highest total intracellular carotenoid level was about  $1000 \text{ mg L}^{-1}$  between 60 and 68 h. The results show that carotenoids are synthesized mainly when cellular growth is inhibited due to depletion of some nutritional ingredients in the culture medium.

Carotenoids are secondary metabolites. As such, their synthesis should be closely correlated with the state of cellular growth and metabolic activity of other common biomolecules within cells, like nucleic acids, proteins, and lipids. Monitoring changes in these substances will improve our understanding of the regulation of carotenogenesis. However, the estimation of protein content using Raman spectroscopy in *R. glutinis* cells is difficult because the Raman peak at  $1005 \text{ cm}^{-1}$ , which is commonly used for protein quantification, coincides with the  $\delta(\text{C}=\text{CH})$  carotenoid band. In this paper, we monitored time-dependent changes in the intensity of the  $783 \text{ cm}^{-1}$  peak (assigned to nucleic acids) and the  $1741 \text{ cm}^{-1}$  peak (assigned to lipids) during the culture process (Fig. 3b). The peak intensity at  $783 \text{ cm}^{-1}$  correlated with the amount of DNA and RNA, which reached a high level in early exponential phase (8–20 h) and subsequently decreased until the lowest value was reached in the late exponential phase (48 h). Most of *R. glutinis* cells in the early exponential phase are in rapid proliferation. In contrast, they are in quiescence in the late exponential and stationary phases. Cells in proliferation have more DNA than those in quiescence due to chromosomal DNA replication. Moreover, the former possess a greater number of ribosomes, which consist of rRNA and proteins, increasing the amount of RNA. Consequently, the fluctuation of the  $783 \text{ cm}^{-1}$  peak intensity reflects the changes in nucleic acids in cells and can be used as a marker for metabolic activity involved in

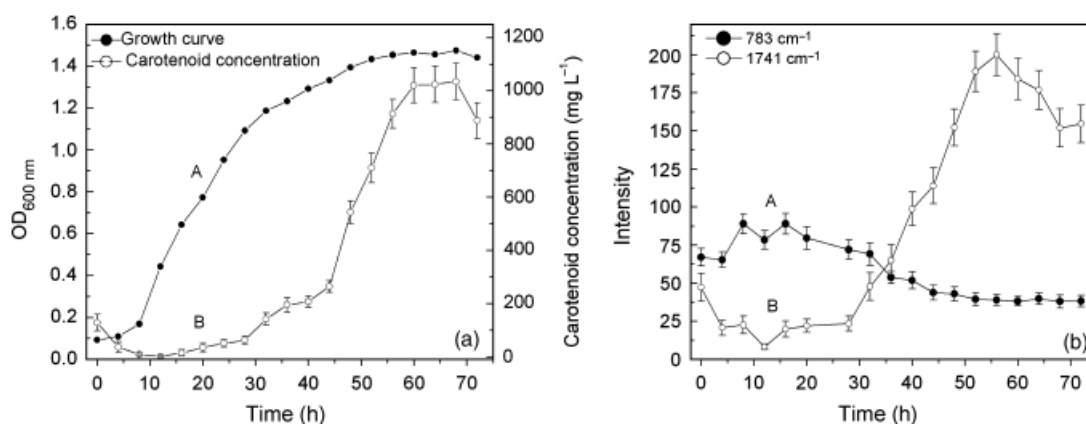


**Fig. 3.** (a) Growth behavior of *Rhodotorula glutinis* (left scale, curve A) and time-dependent changes of carotenoid content in *R. glutinis* cells submerged in culture (right scale, curve B). (b) Time-dependent changes in average intensities of the *R. glutinis* Raman band at  $783 \text{ cm}^{-1}$  (curve A) and  $1741 \text{ cm}^{-1}$  (curve B).

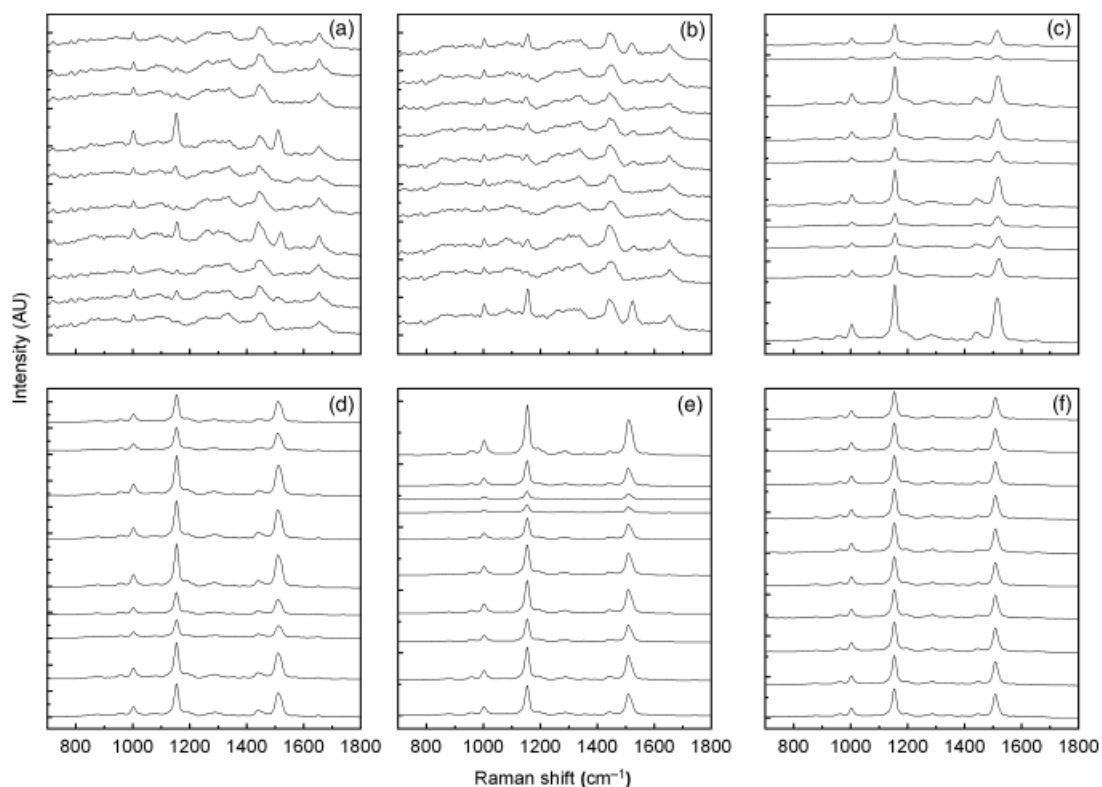


**Fig. 4.** The variation of the carotenoid level in single cells. Ten randomly selected Raman spectra from the 100 spectral data of *Rhodotorula glutinis* cells at 8 h (a), 16 h (b, divided by a factor of 2), 32 h (c, divided by a factor of 5), 48 h (d, divided by a factor of 20), and 64 h (e, divided by a factor of 50); and 100 measurements on a single cell cultured for 64 h (f, divided by a factor of 50).

cellular growth. Figure 3b shows that the profile of changes in the  $1741\text{ cm}^{-1}$  band intensity is similar to that of carotenoid accumulation in *R. glutinis* cells, indicating that the majority of the lipids are synthesized in the late exponential and stationary phases. The changes in carotenoid, nucleic acid, and lipid content within cells may be explained as follows. In the early and middle exponential phases, most cells are in rapid proliferation and large quantities of carbon-based metabolites, like tricarboxylic acid cycle metabolites, are used to generate ATP to meet the energy demands of cellular growth. However, these metabolites accumulate when cellular growth is inhibited due to nutrient depletion in the medium during the late exponential and stationary phases. Thus excessive amounts of metabolites are then converted into other products, including lipids and carotenoids.

### Comparison of LTRS and the traditional HPLC method

This description of time-dependent changes in carotenoid content inside cells of *R. glutinis* when submerged in culture is in agreement with that measured by Bhosale & Gadre

(2001b) using HPLC. However, carotenoid quantification based on LTRS has the following advantages over traditional methods. First, it is less time consuming. The classic extraction procedure using HPLC requires over 5 h. In contrast, it only takes about 40 min to acquire Raman spectra from 100 cells. Second, LTRS cannot cause degradation or isomerization of carotenoids when using a low-power laser. Third, only a small amount of sample, for example, not more than  $200\ \mu\text{L}$  culture, is required for carotenoid measurement. Finally, because no organic solvent is used for LTRS, environmental pollution and health hazards can be avoided.

### Importance of single-cell analytical techniques

Most of our knowledge on the microbial fermentation process has been obtained by inference from cell-population level data, including information on substrate concentration, product concentration, and fermentation broth pH. However, in many cases, a population of cells has a different response to the environment due to heterogeneity within the population. The increasing need to understand individual cell behavior drives the development of single-cell analytical

**Table 2.** Statistical summary of *Rhodotorula glutinis* cell carotenoid content at different time points

Time point (h)	Mean (mg L <sup>-1</sup> )	CV (%)
8	7.6	144
16	13.8	241
32	141.6	63
48	542.9	33
64	1024.1	32
64, single cell*	1087.1	3

\*In this case the carotenoid level in a single cell was measured 100 times to estimate measuring error.

techniques. Of particular importance are techniques, like the one presented in this paper, which will enable us to probe the dynamic changes within an individual cell and the intercellular variability that reveals the underlying mechanisms behind the coordination of multicellular behavior. In this work, we assessed the variation in carotenoid levels per cell over 100 single cells of *R. glutinis* at different time points (8, 16, 32, 48, and 64 h). Figure 4 shows 10 randomly selected Raman spectra from the 100 spectral data of *R. glutinis* cells at each time point and Table 2 illustrates the mean value and coefficient of variation (CV; SD/mean) for carotenoid content inside the cells at these time points. In the lag (8 h) and early exponential phases (16 h), most cells were in rapid proliferation and had a low intracellular carotenoid content. The variation in carotenoid levels of cells was significant, giving a CV value of 144% and 241%, respectively. At 32 h, most cells entered the carotenogenesis phase and the heterogeneity in carotenoid levels began to diminish, with a CV value of 63%. A further decrease of variation in the carotenoid levels of cells could be seen with the increase of the carotenoid content during the late exponential and stationary phases; the CVs were 33% and 32%, respectively. The results indicate that the carotenoid levels in individual cells in a population vary significantly, especially for the population of cells in the lag and early exponential phases. In order to estimate the carotenoid level measurement errors, we made 100 measurements on a single cell randomly selected from the sample at 64 h. The CV was 3%, well below the variation in the carotenoid levels among 100 individual cells from the same sample (CV 32%). This finding shows that cellular heterogeneity, rather than measurement error, is the main source of significant variation. There are various reasons for metabolic heterogeneity, including mutations, random transcription events, and asymmetries in the distribution of nucleic acids and proteins between mother and daughter cells in the process of cellular division (Brehm-Stecher & Johnson, 2004). LTRS may provide further insight into differences in the potential for carotenogenesis for individual cells and what governs it.

## Acknowledgements

This work was supported by National Natural Science Foundation of China (31060128) and Guangxi Natural Science Foundation (0991078 and 0832022z). We thank Ms. Lianzhu Teng at the College of Biological Science, Guangxi University for *R. glutinis* strain.

## References

- Ashkin A, Dziedzic JM & Yamane T (1987) Optical trapping and manipulation of single cells using infrared laser beams. *Nature* **330**: 769–771.
- Baranski R, Baranska M & Schulz H (2005) Changes in carotenoid content and distribution in living plant tissue can be observed and mapped *in situ* using NIR-FT-Raman spectroscopy. *Planta* **222**: 448–457.
- Bernstein PS, Yoshida MD, Katz NB, McClane RW & Gellermann W (1998) Raman detection of macular carotenoid pigments in intact human retina. *Invest Ophthalmol Vis Sci* **39**: 2003–2011.
- Bhosale PB & Gadre RV (2001a) Production of beta-carotene by a mutant of *Rhodotorula glutinis*. *Appl Microbiol Biot* **55**: 423–427.
- Bhosale P & Gadre RV (2001b) Optimization of carotenoid production from hyper-producing *Rhodotorula glutinis* mutant 32 by a factorial approach. *Lett Appl Microbiol* **33**: 12–16.
- Brehm-Stecher BF & Johnson EA (2004) Single-cell microbiology: tools, technologies, and applications. *Microbiol Mol Biol R* **68**: 538–559.
- Buijtelts PC, Willemsse-Erix HF, Petit PL *et al.* (2008) Rapid identification of mycobacteria by Raman spectroscopy. *J Clin Microbiol* **46**: 961–965.
- Chen D, Shelenkova L, Li Y, Kempf CR & Sabelnikov A (2009) Laser tweezers Raman spectroscopy potential for studies of complex dynamic cellular processes: single cell bacterial lysis. *Anal Chem* **81**: 3227–3238.
- Frengova GI & Beshkova DM (2009) Carotenoids from *Rhodotorula* and *Phaffia*: yeasts of biotechnological importance. *J Ind Microbiol Biot* **36**: 163–180.
- Huang SS, Chen D, Pelczar PL, Vepachedu VR, Setlow P & Li YQ (2007) Levels of Ca<sup>2+</sup>-dipicolinic acid in individual bacillus spores determined using microfluidic Raman tweezers. *J Bacteriol* **189**: 4681–4687.
- Kaiser P, Surmann P, Vallentin G & Fuhrmann H (2007) A small-scale method for quantitation of carotenoids in bacteria and yeasts. *J Microbiol Meth* **70**: 142–149.
- Kanter EM, Vargis E, Majumder S, Keller MD, Woeste E, Rao GG & Mahadevan-Jansen A (2009) Application of Raman spectroscopy for cervical dysplasia diagnosis. *J Biophoton* **2**: 81–90.
- Li-Chan ECY (1996) The applications of Raman spectroscopy in food science. *Trends Food Sci Technol* **7**: 361–370.
- Nottingham I, Verrier S, Haque S, Polak JM & Hench LL (2003) Spectroscopic study of human lung epithelial cells (A549) in culture: living cells versus dead cells. *Biopolymers* **72**: 230–240.

- Ojeda JF, Xie C, Li YQ, Bertrand FE, Wiley J & McConnell TJ (2006) Chromosomal analysis and identification based on optical tweezers and Raman spectroscopy. *Opt Express* **14**: 5385–5393.
- Papaioannou EH, Liakopoulou-Kyriakides M, Christofilos D, Arvanitidis I & Kourouklis G (2009) Raman spectroscopy for intracellular monitoring of carotenoid in *blakeslea trispora*. *Appl Biochem Biotech* **159**: 478–487.
- Rousseau ME, Lefevre T, Beaulieu L, Asakura T & Pezolet M (2004) Study of protein conformation and orientation in silkworm and spider silk fibers using Raman microspectroscopy. *Biomacromolecules* **5**: 2247–2257.
- Sakaki H, Nochide H, Komemushi S & Miki W (2002) Effect of active oxygen species on the productivity of torularhodin by *Rhodotorula glutinis* No. 21. *J Biosci Bioeng* **93**: 338–340.
- Schulz H, Baranska M & Baranski R (2005) Potential of NIR-FT-Raman spectroscopy in natural carotenoid analysis. *Biopolymers* **77**: 212–221.
- Simpson KL, Nakayama TO & Chichester CO (1964) Biosynthesis of yeast carotenoids. *J Bacteriol* **88**: 1688–1694.
- Snook RD, Harvey TJ, Correia Faria E & Gardner P (2009) Raman tweezers and their application to the study of singly trapped eukaryotic cells. *Integr Biol (Cambridge)* **1**: 43–52.
- Tang H, Yao H, Wang G, Wang Y, Li YQ & Feng M (2007) NIR Raman spectroscopic investigation of single mitochondria trapped by optical tweezers. *Opt Express* **15**: 12708–12716.
- Tereshina VM, Memorskaia AS & Feofilova EP (2003) Zygote formation in *Blakeslea trispora*: morphological peculiarities and relationship with carotenoid synthesis. *Mikrobiologiya* **72**: 503–509.
- Vitek P, Jehlicka J, Edwards HG & Osterrothova K (2009) Identification of beta-carotene in an evaporitic matrix – evaluation of Raman spectroscopic analysis for astrobiological research on Mars. *Anal Bioanal Chem* **393**: 1967–1975.
- Wang SL, Sun JS, Han BZ & Wu XZ (2007) Optimization of beta-carotene production by *Rhodotorula glutinis* using high hydrostatic pressure and response surface methodology. *J Food Sci* **72**: M325–M329.
- Xie C, Dinno MA & Li Y-q (2002) Near-infrared Raman spectroscopy of single optically trapped biological cells. *Opt Lett* **27**: 249–251.
- Xie C, Mace J, Dinno MA, Li YQ, Tang W, Newton RJ & Gemperline PJ (2005) Identification of single bacterial cells in aqueous solution using confocal laser tweezers Raman spectroscopy. *Anal Chem* **77**: 4390–4397.
- Xie C, Nguyen N, Zhu Y & Li YQ (2007) Detection of the recombinant proteins in single transgenic microbial cell using laser tweezers and Raman spectroscopy. *Anal Chem* **79**: 9269–9275.
- Xu Y (2005) *Raman Spectroscopy in Application of Structural Biology*. Chemical Industry Press, Beijing.